EURASIP Journal on Applied Signal Processing 2003:13, 1279–1290

Efficient Channel Shortening Equalizer Design

Richard K. Martin
School of Electrical and Computer Engineering, Cornell University, Ithaca, NY 14853, USA
Email: frodo@ece.cornell.edu

Ming Ding
Department of Electrical and Computer Engineering, The University of Texas at Austin, Austin, TX 78712-1084, USA
Email: ming@ece.utexas.edu

Brian L. Evans
Department of Electrical and Computer Engineering, The University of Texas at Austin, Austin, TX 78712-1084, USA
Email: bevans@ece.utexas.edu

C. Richard Johnson Jr.
School of Electrical and Computer Engineering, Cornell University, Ithaca, NY 14853, USA
Email: johnson@ece.cornell.edu

Received 6 February 2003 and in revised form 9 June 2003

Time-domain equalization is crucial in reducing channel state dimension in maximum likelihood sequence estimation and intercarrier and intersymbol interference in multicarrier systems. A time-domain equalizer (TEQ) placed in cascade with the channel produces an effective impulse response that is shorter than the channel impulse response. This paper analyzes two TEQ design methods amenable to cost-effective real-time implementation: minimum mean square error (MMSE) and maximum shortening SNR (MSSNR) methods. We reduce the complexity of computing the matrices in the MSSNR and MMSE designs by a factor of 140 and a factor of 16 (respectively) relative to existing approaches, without degrading performance. We prove that an infinite-length MSSNR TEQ with unit norm TEQ constraint is symmetric. A symmetric TEQ halves FIR implementation complexity, enables parallel training of the frequency-domain equalizer and TEQ, reduces TEQ training complexity by a factor of 4, and doubles the length of the TEQ that can be designed using fixed-point arithmetic, with only a small loss in bit rate. Simulations are presented for designs with a symmetric TEQ or target impulse response.

Keywords and phrases: multicarrier modulation, channel shortening, time-domain equalization, efficient computation, symmetry.

1. INTRODUCTION

Channel shortening, a generalization of equalization, has recently become necessary in receivers employing multicarrier modulation (MCM) [1]. MCM techniques like orthogonal frequency division multiplexing (OFDM) and discrete multitone (DMT) have been deployed in applications such as the wireless LAN standards IEEE 802.11a and HIPERLAN/2, digital audio broadcast (DAB) and digital video broadcast (DVB) in Europe, and asymmetric and very-high-speed digital subscriber loops (ADSL, VDSL). MCM is attractive due to the ease with which it can combat channel dispersion, provided that the channel delay spread is not greater than the length of the cyclic prefix (CP). However, if CP is not long enough, the orthogonality of the subcarriers is lost, causing intercarrier interference (ICI) and intersymbol interference (ISI).

A well-known technique to combat the ICI/ISI caused by the inadequate CP length is the use of a time-domain equalizer (TEQ) in the receiver front end. The TEQ is a finite impulse response filter that shortens the channel so that the delay spread of the combined channel-equalizer impulse response is not longer than the CP length. The TEQ design problem has been extensively studied in the literature [2, 3, 4, 5, 6, 7, 8, 9, 10, 11, 12]. In [3], Falconer and Magee proposed a minimum mean square error (MMSE) method for channel shortening, which was designed to reduce the complexity in maximum likelihood sequence estimation (MLSE). More recently, Melsa et al. [5] proposed the maximum shortening SNR (MSSNR) method, which attempts to minimize the energy outside the window of interest while holding the energy inside fixed. This approach was generalized to the min-ISI method in [9], which allows the

residual ISI to be shaped in the frequency domain. A blind, adaptive algorithm that searches for the TEQ maximizing the SSNR cost function was proposed in [10].

Channel shortening has also applications in MLSE [13] and multiuser detection [14]. For MLSE, for an alphabet of size $\mathcal{A}$ and an effective channel length of $L_c + 1$, the complexity of MLSE grows as $\mathcal{A}^{L_c}$ grows. One method of reducing this enormous complexity is to employ a prefilter to shorten the channel to a manageable length [2, 3]. Similarly, in a multiuser system with a flat fading channel for each user, the optimum detector is the MLSE, yet complexity grows exponentially with the number of users. "Channel shortening" can be implemented to suppress a specified number of the scalar channels, effectively reducing the number of users to be detected by the MLSE [14]. In this context, "channel shortening" means reducing the number of scalar channels rather than reducing the number of channel taps. In this paper, we focus on channel shortening for ADSL systems, but the same designs can be applied to channel shortening for the MLSE and for multiuser detectors.

This paper examines the MSSNR and MMSE methods of channel shortening. The structure of each solution is exploited to dramatically reduce the complexity of computing the TEQ. Previous work on reducing the complexity of the MSSNR design was presented in [8]. This work exploited the fact that the matrices involved are almost Toeplitz, so the $(i + 1, j + 1)$ element can be computed efficiently from the (i, j) element. Our proposed method makes use of this, but focuses rather on determining the matrices and eigenvector for a given delay based on the matrices and eigenvector computed for the previous delay.

In addition, we examine exploiting symmetry in the TEQ and in the target impulse response (TIR). In [15], it was shown that the MSSNR TEQ and the MMSE TIR were approximately symmetric. In [16, 17], simulations were presented for algorithms that forced the MSSNR TEQ to be perfectly symmetric or skew-symmetric. This paper proves that the infinite-length MSSNR TEQ with a unit norm constraint on the TEQ is perfectly symmetric. We show how to exploit this symmetry in computing the MMSE TIR, adaptively computing the MSSNR TEQ, and in computing the frequency-domain equalizer (FEQ) in parallel with the TEQ.

The remainder of this paper is organized as follows. Section 2 presents the system model and notation. Section 3 reviews the MSSNR and MMSE designs. Section 4 discusses methods of reducing the computation of each design without performance loss. Section 5 examines symmetry in the impulse response and Section 6 shows how to exploit this symmetry to further reduce the complexity, though with a possible small performance loss. Section 7 provides simulation results and Section 8 concludes the paper.

2. SYSTEM MODEL AND NOTATION

The multicarrier system model is shown in Figure 1 and the notation is summarized in Table 1. Each block of bits is divided up into N bins and each bin is viewed as a QAM signal that will be modulated by a different carrier. An efficient means of implementing the multicarrier modulation in discrete time is to use an inverse fast Fourier transform (IFFT). The IFFT converts each bin (which acts as one of the frequency components) into a time-domain signal. After transmission, the receiver can use an FFT to recover the data within a bit error rate tolerance, provided that equalization has been performed properly.

Table 1: Channel shortening notation.

Notation	Meaning
$x(k)$	Transmitted signal (IFFT output)
$n(k)$	Channel noise
$r(k)$	Received signal
$y(k)$	Signal after TEQ
N, ν	Sizes of FFT and CP
Δ	Desired delay (design parameter)
N_Δ	Number of possible values of Δ
$\mathbf{h} = [h_0, \ldots, h_{L_h}]$	Channel impulse response
$\mathbf{w} = [w_0, \ldots, w_{L_w}]$	TEQ impulse response
$\mathbf{c} = [c_0, \ldots, c_{L_c}]$	Effective channel ($\mathbf{c} = \mathbf{h} \star \mathbf{w}$)
$\mathbf{b} = [b_0, \ldots, b_\nu]$	Target impulse response
$\tilde{L}_h = L_h + 1$	Channel length
$\tilde{L}_w = L_w + 1$	TEQ length
$\tilde{L}_c = L_c + 1$	Length of the effective channel
$\mathbf{H}$	$\tilde{L}_c \times \tilde{L}_w$ channel convolution matrix
$\mathbf{H}_{\text{win}}(\Delta)$	Rows Δ through $\Delta + \nu$ of $\mathbf{H}$
$\mathbf{H}_{\text{wall}}(\Delta)$	$\mathbf{H}$ with rows Δ through $\Delta + \nu$ removed
$\mathbf{I}_N$	$N \times N$ identity matrix
$[\mathbf{A}]_{(i,j)}$	Element i, j of matrix $\mathbf{A}$
$\mathbf{A}^*$, $\mathbf{A}^T$, $\mathbf{A}^H$	Conjugate, transpose, and Hermitian

In order for the subcarriers to be independent, the convolution of the signal and the channel must be a circular convolution. It is actually a linear convolution, so it is made to appear circular by adding a CP to the start of each data block. The CP is obtained by prepending the last ν samples of each block to the beginning of the block. If the CP is at least as long as the channel, then the output of each subchannel is equal to the input times a scalar complex gain factor. The signals in the bins can then be equalized by a bank of complex gains, referred to as FEQ [18].

The above discussion assumes that CP length +1 is greater than or equal to the channel length. However, transmitting the CP wastes time slots that could be used to transmit data. Thus, the CP is usually set to a reasonably small value, and a TEQ is employed to shorten the channel to this length. In ADSL and VDSL, the CP length is 1/16 of the block (symbol) length. As discussed in Section 1, TEQ design methods have been well explored [2, 3, 4, 5, 6, 7, 8, 9, 10, 11, 12].

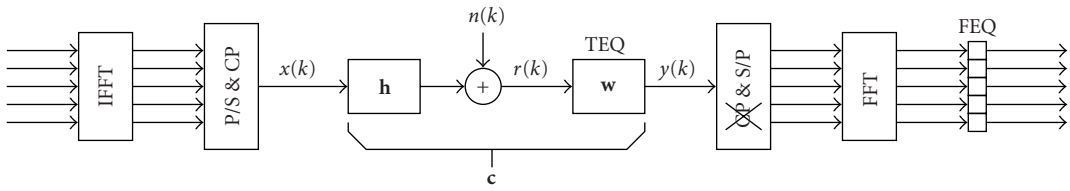

Figure 1: Traditional multicarrier system model. (I)FFT: (inverse) fast Fourier transform, P/S: parallel to serial, S/P: serial to parallel, CP: add cyclic prefix, and crossed CP: remove cyclic prefix.

One of the TEQ's main burdens, in terms of computational complexity, is due to the parameter Δ, which is the desired delay of the effective channel. The performance of most TEQ designs does not vary smoothly with delay [19], hence a global search over delay is required in order to compute an optimal design. Since the effective channel has $L_c + 1$ taps, there are $L_c + 1 - \nu$ locations in which one can place a window of length $\nu+1$ of nonzero taps, hence $0 \le \Delta \le L_c - \nu$. For typical downstream ADSL parameters, this means there are about 500 delay values to examine, and an optimal solution must be computed for each one. One of the goals of this paper is to show how to reuse computations from each value of Δ to reduce the computational cost for the following value of Δ, which greatly reduces the overall computational burden.

3. REVIEW OF THE MSSNR AND MMSE DESIGNS

This section reviews the MSSNR and MMSE designs for channel shortening.

3.1. The MSSNR solution

Consider MSSNR TEQ design [5]. This technique attempts to maximize the ratio of the energy in a window of the effective channel over the energy in the remainder of the effective channel. Following [5], we define

$$\mathbf{H}_{\text{win}} = \begin{bmatrix} h(\Delta) & h(\Delta-1) & \cdots & h(\Delta-\tilde{L}_w+1) \\ \vdots & \vdots & \ddots & \vdots \\ h(\Delta+\nu) & h(\Delta+\nu-1) & \cdots & h(\Delta+\nu-\tilde{L}_w+1) \end{bmatrix}, \tag{1}$$

$$\mathbf{H}_{\text{wall}} = \begin{bmatrix} h(0) & 0 & \cdots & 0 \\ \vdots & \ddots & & \vdots \\ h(\Delta-1) & h(\Delta-2) & \cdots & h(\Delta-\tilde{L}_w) \\ h(\Delta+\nu+1) & h(\Delta+\nu) & \cdots & h(\Delta+\nu-\tilde{L}_w+2) \\ \vdots & \ddots & & \vdots \\ 0 & \cdots & 0 & h(L_h) \end{bmatrix}. \tag{2}$$

Thus, $\mathbf{c}_{\text{win}} = \mathbf{H}_{\text{win}}\mathbf{w}$ yields a window of length $\nu + 1$ of the effective channel, and $\mathbf{c}_{\text{wall}} = \mathbf{H}_{\text{wall}}\mathbf{w}$ yields the remainder of the effective channel. The MSSNR design problem can be stated as "minimize $\|\mathbf{c}_{\text{wall}}\|$ subject to the constraint $\|\mathbf{c}_{\text{win}}\| = 1$," as in [5]. This reduces to

$$\min_{\mathbf{w}} (\mathbf{w}^T\mathbf{A}\mathbf{w}) \quad \text{subject to } \mathbf{w}^T\mathbf{B}\mathbf{w} = 1, \tag{3}$$

where

$$\mathbf{A} = \mathbf{H}_{\text{wall}}^T\mathbf{H}_{\text{wall}}, \qquad \mathbf{B} = \mathbf{H}_{\text{win}}^T\mathbf{H}_{\text{win}}. \tag{4}$$

The $\tilde{L}_w \times \tilde{L}_w$ matrices $\mathbf{A}$ and $\mathbf{B}$ are real and symmetric. However, $\mathbf{A}$ is invertible, but $\mathbf{B}$ may not be [20]. An alternative formulation that addresses this is to "maximize $\|\mathbf{c}_{\text{win}}\|$ subject to the constraint $\|\mathbf{c}_{\text{wall}}\| = 1$," [20] which works well even when $\mathbf{B}$ is not invertible. The alternative formulation reduces to

$$\max_{\mathbf{w}} (\mathbf{w}^T\mathbf{B}\mathbf{w}) \quad \text{subject to } \mathbf{w}^T\mathbf{A}\mathbf{w} = 1, \tag{5}$$

where $\mathbf{A}$ and $\mathbf{B}$ are defined in (4). Solving (3) leads to a TEQ that satisfies the generalized eigenvector problem

$$\mathbf{A}\mathbf{w} = \tilde{\lambda}\mathbf{B}\mathbf{w}, \tag{6}$$

and the alternative formulation in (5) leads to a related generalized eigenvector problem

$$\mathbf{B}\mathbf{w} = \lambda\mathbf{A}\mathbf{w}. \tag{7}$$

The solution for $\mathbf{w}$ will be the generalized eigenvector corresponding to the smallest (largest) generalized eigenvalue $\tilde{\lambda}$ (λ), respectively. Section 4 shows how to obtain most of $\mathbf{B}(\Delta+1)$ from $\mathbf{B}(\Delta)$, how to obtain $\mathbf{A}(\Delta)$ from $\mathbf{B}(\Delta)$, and how to initialize the eigensolver for $\mathbf{w}(\Delta+1)$ based on the solution for $\mathbf{w}(\Delta)$.

3.2. The MMSE solution

The system model for the MMSE solution [3] is shown in Figure 2. It creates a virtual TIR $\mathbf{b}$ of length $\nu + 1$ such that the MSE, which is measured between the output of the effective channel and the output of the TIR, is minimized. In the absence of noise, if the input signal is white, then the optimal MMSE and MSSNR solutions are identical [6]. A unified treatment of the MSSNR and noisy MMSE solutions was given in [15].

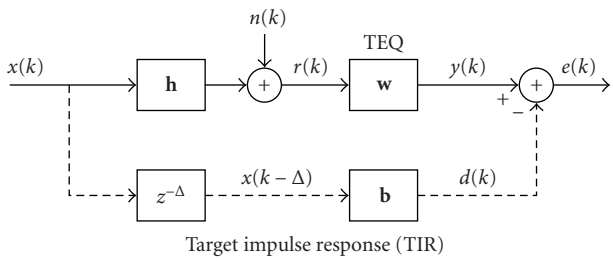

FIGURE 2: MMSE system model. The symbols **h**, **w**, and **b** are the impulse responses of the channel, the TEQ, and the target, respectively. Here, Δ represents transmission delay. The dashed lines indicate a virtual path, which is used only for analysis.

The MMSE design uses a TIR **b** that must satisfy [2]

$$\mathbf{R}_{rx}\mathbf{b} = \mathbf{R}_r\mathbf{w}, \tag{8}$$

where

$$\mathbf{R}_{rx} = E\left[\begin{bmatrix} r(k) \\ \vdots \\ r(k-L_w) \end{bmatrix}\begin{bmatrix} x(k-\Delta) & \cdots & x(k-\Delta-\nu) \end{bmatrix}\right] \tag{9}$$

is the channel input-output cross-correlation matrix and

$$\mathbf{R}_r = E\left[\begin{bmatrix} r(k) \\ \vdots \\ r(k-L_w) \end{bmatrix}\begin{bmatrix} r(k) & \cdots & r(k-L_w) \end{bmatrix}\right] \tag{10}$$

is the channel output autocorrelation matrix. Typically, **b** is computed first, and then (8) is used to determine **w**. The goal is that $\mathbf{h} \star \mathbf{w}$, the convolution of **h** and **w**, approximates a delayed version of **b**. The TIR is the eigenvector corresponding to the minimum eigenvalue of [3, 4, 7]

$$\mathbf{R}(\Delta) = \mathbf{R}_x - \mathbf{R}_{xr}\mathbf{R}_r^{-1}\mathbf{R}_{rx}. \tag{11}$$

Section 4 addresses how to determine most of $\mathbf{R}(\Delta+1)$ from $\mathbf{R}(\Delta)$, and how to use the solution for $\mathbf{b}(\Delta)$ to initialize the eigensolver for $\mathbf{b}(\Delta+1)$.

4. EFFICIENT COMPUTATION

There is a tremendous amount of redundancy involved in the brute force calculation of the MSSNR design. This has been addressed in [8]. This section discusses methods of reusing even more of the computations to dramatically decrease the required complexity. Specifically, for a given delay Δ,

(1) $\mathbf{A}(\Delta)$ can be computed from $\mathbf{B}(\Delta)$ almost for free,
(2) $\mathbf{B}(\Delta+1)$ can be computed from $\mathbf{B}(\Delta)$ almost for free,
(3) a shifted version of the optimal MSSNR TEQ $\mathbf{w}(\Delta)$ can be used to initialize the generalized eigenvector solution for $\mathbf{w}(\Delta+1)$ to decrease the number of iterations needed for the eigenvector computation,
(4) $\mathbf{R}(\Delta+1)$ can be computed from $\mathbf{R}(\Delta)$ almost for free,
(5) a shifted version of the optimal MMSE TIR $\mathbf{b}(\Delta)$ can be used to initialize the generalized eigenvector solution for $\mathbf{b}(\Delta+1)$ to decrease the number of iterations needed for the eigenvector computation.

We now discuss each of these points in turn.

4.1. *Computing* $\mathbf{A}(\Delta)$ *from* $\mathbf{B}(\Delta)$

Let $\mathbf{C} = \mathbf{H}^T\mathbf{H}$ and recall that $\mathbf{A} = \mathbf{H}_{\text{wall}}^T\mathbf{H}_{\text{wall}}$ and $\mathbf{B} = \mathbf{H}_{\text{win}}^T\mathbf{H}_{\text{win}}$. Note that

$$\mathbf{H} = \begin{bmatrix} \mathbf{H}_1 \\ \mathbf{H}_{\text{win}} \\ \mathbf{H}_2 \end{bmatrix}, \qquad \mathbf{H}_{\text{wall}} = \begin{bmatrix} \mathbf{H}_1 \\ \mathbf{H}_2 \end{bmatrix}. \tag{12}$$

Thus,

$$\begin{aligned} \mathbf{C} &= \mathbf{H}_1^T\mathbf{H}_1 + \mathbf{H}_{\text{win}}^T\mathbf{H}_{\text{win}} + \mathbf{H}_2^T\mathbf{H}_2 \\ &= \underbrace{\left(\mathbf{H}_1^T\mathbf{H}_1 + \mathbf{H}_2^T\mathbf{H}_2\right)}_{\mathbf{A}} + \underbrace{\left(\mathbf{H}_{\text{win}}^T\mathbf{H}_{\text{win}}\right)}_{\mathbf{B}}. \end{aligned} \tag{13}$$

To emphasize the dependence on the delay Δ, we write

$$\mathbf{C} = \mathbf{A}(\Delta) + \mathbf{B}(\Delta). \tag{14}$$

Since **C** is symmetric and Toeplitz, it is fully determined by its first row or column:

$$\mathbf{C}_{(0:L_w,0)} = \mathbf{H}^T\left[\mathbf{h}^T, \mathbf{0}_{(1\times L_w)}\right]^T = \left(\mathbf{H}_{(0:L_h,0:L_w)}\right)^T\mathbf{h}. \tag{15}$$

Thus, **C** can be computed using less than $\tilde{L}_h^2$ multiply-adds and its first column can be stored using $\tilde{L}_w$ memory words. Since **C** is independent of Δ, we only need to compute it once. Then each time Δ is incremented and the new $\mathbf{B}(\Delta)$ is computed, $\mathbf{A}(\Delta)$ can be computed from $\mathbf{A}(\Delta) = \mathbf{C} - \mathbf{B}(\Delta)$ using only $\tilde{L}_w^2$ additions and no multiplications. In contrast, the "brute force" method requires $\tilde{L}_w^2(L_h - \nu)$ multiply-adds per delay, and the method of [8] requires about $\tilde{L}_w(L_w + L_h - \nu)$ multiply-adds per delay.

4.2. *Computing* $\mathbf{B}(\Delta+1)$ *from* $\mathbf{B}(\Delta)$

Recall that $\mathbf{B}(\Delta) = \mathbf{H}_{\text{win}}^T(\Delta)\mathbf{H}_{\text{win}}(\Delta)$, where $\mathbf{H}_{\text{win}}(\Delta)$ is defined as in (1).

The key observation is that

$$\left[\mathbf{H}_{\text{win}}(\Delta+1)\right]_{(0:\nu,\,1:L_w)} = \left[\mathbf{H}_{\text{win}}(\Delta)\right]_{(0:\nu,\,0:L_w-1)}. \tag{16}$$

This means that

$$\left[\mathbf{B}(\Delta+1)\right]_{(1:L_w,\,1:L_w)} = \left[\mathbf{B}(\Delta)\right]_{(0:L_w-1,\,0:L_w-1)}, \tag{17}$$

so most of $\mathbf{B}(\Delta+1)$ can be obtained without requiring any computations. Now, partition $\mathbf{B}(\Delta+1)$ as

$$\mathbf{B}(\Delta+1)=\begin{bmatrix}\alpha & \mathbf{g}^T\\ \mathbf{g} & \hat{\mathbf{B}}\end{bmatrix}, \tag{18}$$

where $\hat{\mathbf{B}}$ is obtained from (17). Since $\mathbf{B}(\Delta+1)$ is almost Toeplitz, α and all of the elements of $\mathbf{g}$ save the last can be efficiently determined from the first column of $\hat{\mathbf{B}}$ [8]. Computing each of these L_w elements requires two multiply-adds. Finally, to compute the last element of $\mathbf{g}$,

$$\mathbf{g}_{L_w}=\left([\mathbf{H}_{\text{win}}]_{(0:\nu,L_w)}\right)^T[\mathbf{H}_{\text{win}}]_{(0:\nu,0)}, \tag{19}$$

$\nu+1$ multiply-adds are required.

4.3. Computing $\mathbf{R}(\Delta+1)$ from $\mathbf{R}(\Delta)$

Recall that for the MMSE design, we must compute

$$\mathbf{R}(\Delta)=\mathbf{R}_x-\mathbf{R}_{xr}\mathbf{R}_r^{-1}\mathbf{R}_{rx}, \tag{20}$$

where

$$\begin{aligned}\mathbf{R}_x&=E[\mathbf{x}_k\,\mathbf{x}_k^T],\\ \mathbf{R}_{rx}&=E[\mathbf{r}_k\,\mathbf{x}_k^T],\\ \mathbf{x}_k&=\left[x(k-\Delta),\ \ldots,\ x(k-\Delta-\nu)\right]^T,\\ \mathbf{r}_k&=\left[r(k),\ \ldots,\ x(k-L_w)\right]^T.\end{aligned} \tag{21}$$

Note that $\mathbf{R}_x$ does not depend on Δ and is Toeplitz. Thus,

$$\begin{aligned}[\mathbf{R}_x(\Delta+1)]_{(0:\nu-1,\,0:\nu-1)}&=[\mathbf{R}_x(\Delta)]_{(0:\nu-1,\,0:\nu-1)}\\ &=[\mathbf{R}_x(\Delta)]_{(1:\nu,\,1:\nu)}.\end{aligned} \tag{22}$$

Let $\mathbf{P}(\Delta)=\mathbf{R}_{xr}\mathbf{R}_r^{-1}\mathbf{R}_{rx}$. Observing that

$$[\mathbf{R}_{rx}(\Delta+1)]_{(0:L_w,\,0:\nu-1)}=[\mathbf{R}_{rx}(\Delta)]_{(0:L_w,\,1:\nu)}, \tag{23}$$

we see that

$$[\mathbf{P}(\Delta+1)]_{(0:\nu-1,\,0:\nu-1)}=[\mathbf{P}(\Delta)]_{(1:\nu,\,1:\nu)}. \tag{24}$$

Combining (22) and (24),

$$[\mathbf{R}(\Delta+1)]_{(0:\nu-1,\,0:\nu-1)}=[\mathbf{R}(\Delta)]_{(1:\nu,\,1:\nu)}. \tag{25}$$

The matrix $\mathbf{R}_r$ is symmetric and Toeplitz. However, the inverse of a Toeplitz matrix is, in general, not Toeplitz [21]. This means that $\mathbf{R}(\Delta)$ has no further structure that can be easily exploited, so the first row and column of $\mathbf{R}(\Delta+1)$ cannot be obtained from the rest of $\mathbf{R}(\Delta+1)$ using the tricks in [8]. Even so, (25) allows us to obtain most of the elements of each $\mathbf{R}(\Delta)$ for free, so only $\nu+1$ elements must be computed rather than $(\nu+1)(\nu+2)/2$ elements. In ADSL, $\nu=32$; in VDSL, ν can range up to 512; and in DVB, ν can range up to 2048. Thus, the proposed method reduces the complexity of calculating $\mathbf{R}(\Delta)$ by factors of 17, 257, and 1025 (respectively) for these standards.

4.4. Intelligent eigensolver initialization

Let $\mathbf{w}(\Delta)$ be the MSSNR solution for a given delay. If we were to increase the allowable filter length by 1, then it follows that

$$\hat{\mathbf{w}}(\Delta+1)=z^{-1}\mathbf{w}(\Delta)=\left[0,\mathbf{w}^T(\Delta)\right]^T \tag{26}$$

should be a near-optimum solution, since it produces the same value of the shortening SNR as for the previous delay. From experience, we suggest that the TEQ coefficients are small near the edges, so the last tap can be removed without drastically affecting the performance. Therefore,

$$\hat{\mathbf{w}}(\Delta+1)=\left[0,\left[\mathbf{w}^T(\Delta)\right]_{(0:L_w-1)}\right]^T \tag{27}$$

is a fairly good solution for the delay $\Delta+1$, so this should be the initialization for the generalized eigenvector solver for the next delay. Similarly, for the MMSE TIR,

$$\hat{\mathbf{b}}(\Delta+1)=\left[0,\left[\mathbf{b}^T(\Delta)\right]_{(0:\nu-1)}\right]^T \tag{28}$$

should be the initialization for the eigenvector solver for the next delay.

4.5. Complexity comparison

Table 2 shows the (approximate) number of computations for each step of the MSSNR method, using the "brute force" approach, the method in [8], and the proposed approach. Note that N_Δ refers to the number of values of the delay that are possible (usually equal to the length of the effective channel minus the CP length). For a typical downstream ADSL system, the parameters are $\tilde{L}_w=L_w+1=32$, $\tilde{L}_h=L_h+1=512$, $L_c=L_w+L_h=542$, $\nu=32$, and $N_\Delta=\tilde{L}_c-\nu=511$. The "example" lines in Table 2 show the required complexity for computing all of the $\mathbf{A}$'s and $\mathbf{B}$'s for these parameters using each approach. Observe that [8] beats the brute force method by a factor of 29, the proposed method beats [8] by a factor of 140, and the proposed method beats the brute force method by a factor of 4008.

Table 3 shows the (approximate) computational requirements of the "brute force" approach and the proposed approach for computing the matrices $\mathbf{R}(\Delta)$, $\Delta\in\{\Delta_{\min},\ldots,\Delta_{\max}\}$. The "example" line shows the required complexity for computing the $\mathbf{R}(\Delta)$ matrices using each method for the same parameter values as the example in Table 2. The proposed method yields a decrease in complexity by a factor of the channel shortener length over two, which in this case is a factor of 16.

It is also interesting to compare the complexity of the MSSNR design to that of the MMSE design. There are several steps that add to the complexity: the computation of the matrices $\mathbf{A}$, $\mathbf{B}$, and $\mathbf{R}(\Delta)$, as addressed in Tables 2 and 3; and the computation of the eigenvector or generalized eigenvector corresponding to the minimum eigenvalue of $\mathbf{R}(\Delta)$ or minimum generalized eigenvalue of $(\mathbf{A},\mathbf{B})$. If "brute force"

Table 2: Computational complexity of various MSSNR implementations. MACs are real multiply-and-accumulates and adds are real additions (or subtractions).

Step	Brute force MACs	Wu et al. [8] MACs	Proposed MACs	Proposed adds
$\mathbf{C}$	0	0	$\tilde{L}_h\tilde{L}_w$	0
$\mathbf{B}(\Delta_{\min})$	$\tilde{L}_w^2(\nu+1)$	$\tilde{L}_w(L_w+\nu)$	$\tilde{L}_w(L_w+\nu)$	0
$\mathbf{A}(\Delta_{\min})$	$\tilde{L}_w^2(L_h-\nu)$	$\tilde{L}_w(L_c-\nu)$	0	$\tilde{L}_w^2$
Each $\mathbf{B}(\Delta)$	$\tilde{L}_w^2(\nu+1)$	$\tilde{L}_w(L_w+\nu)$	$2L_w+\nu+1$	0
Each $\mathbf{A}(\Delta)$	$\tilde{L}_w^2(L_h-\nu)$	$\tilde{L}_w(L_c-\nu)$	0	$\tilde{L}_w^2$
Total	$\tilde{L}_w^2\tilde{L}_hN_\Delta$	$\tilde{L}_w(L_w+L_c)N_\Delta$	$(2\tilde{L}_w+\nu)(N_\Delta-1)+\tilde{L}_h\tilde{L}_w$	$\tilde{L}_w^2N_\Delta$
Example	267,911,168	9,369,696	66,850	523,264

Table 3: Computational complexity of various MMSE implementations. MACs are real multiply-and-accumulates.

Step	Brute force MACs	Proposed MACs
$\mathbf{R}(\Delta_{\min})$	$\tilde{L}_w^3$	$\tilde{L}_w^3$
Each $\mathbf{R}(\Delta)$	$\tilde{L}_w^3$	$2\tilde{L}_w^2$
Total	$N_\Delta\tilde{L}_w^3$	$\tilde{L}_w^2(2(N_\Delta-1)+\tilde{L}_w)$
Example	16,744,448	1,077,248

designs are used, then the computation of the MSSNR matrices costs $L_h/\tilde{L}_w$ times more than the computation of the MMSE matrices, or 16 times more in the example; and if the proposed methods are used, then the computation of the MSSNR matrices costs roughly $(2\tilde{L}_w+\nu)/2\tilde{L}_w^2$ times as much as the computation of the MMSE matrices, or 16 times *less* in the example. However, both solutions also require the computation of an eigenvector for each delay, and the cost of this step depends heavily on both the type of eigensolver used and the values of the matrices involved, so an explicit comparison cannot be made.

5. SYMMETRY IN THE IMPULSE RESPONSE

This section discusses symmetry in the TEQ impulse response. It is shown that the MSSNR TEQ with a unit-norm constraint on the TEQ will become symmetric as the TEQ length goes to infinity, and that in the finite length case, the asymptotic result is approached quite rapidly.

5.1. Finite-length symmetry trends

Consider the MSSNR problem of (3), in which the all-zero solution was avoided by using the constraint $\|\mathbf{c}_{\text{win}}\| = 1$. However, some MSSNR designs use the alternative constraint $\|\mathbf{w}\| = 1$. For example, in [22], an iterative algorithm is proposed which performs a gradient descent of $\|\mathbf{c}_{\text{wall}}\|^2$. Although it is not mentioned in [22], this algorithm needs a constraint to prevent the trivial solution $\mathbf{w} = \mathbf{0}$. A natural constraint is to maintain $\|\mathbf{w}\| = 1$, which can be implemented by renormalizing $\mathbf{w}$ after each iteration. Similarly, a blind, adaptive algorithm was proposed in [10], which is a stochastic gradient descent on $\|\mathbf{c}_{\text{wall}}\|^2$, although it leads to a window of size ν instead of $\nu+1$. (In this case, $\mathbf{A}$ still has the same size, but the elements may be slightly different.) For these two algorithms, the solution must satisfy

$$\min_{\mathbf{w}} (\mathbf{w}^T\mathbf{A}\mathbf{w}) \text{ subject to } \mathbf{w}^T\mathbf{w} = 1. \tag{29}$$

This leads to a TEQ that must satisfy a traditional eigenvector problem

$$\mathbf{A}\mathbf{w} = \lambda\mathbf{w}. \tag{30}$$

In this case, the solution is the eigenvector corresponding to the smallest eigenvalue. Henceforth, we will refer to the solution of (30) as the MSSNR unit norm TEQ (MSSNR-UNT) solution.

A centrosymmetric matrix has the property that when rotated 180° (i.e., flip each element over the center of the matrix), it is unchanged. If a matrix is symmetric and Toeplitz (constant along each diagonal), then it is also centrosymmetric [21]. By inspecting the structure of $\mathbf{A}$, it is easy to see that it is symmetric, and nearly Toeplitz. (In fact, the near-Toeplitz structure is the idea behind the fast algorithms in [8], in which $\mathbf{A}_{i+1,j+1}$ is computed from $\mathbf{A}_{i,j}$ with a small tweak.) Hence, $\mathbf{A}$ is approximately a symmetric centrosymmetric matrix. The eigenvectors of such matrices are either symmetric or skew-symmetric, and in special cases the eigenvector corresponding to the smallest eigenvalue is symmetric [23, 24, 25]. Thus, we expect the MSSNR-UNT TEQ to be approximately symmetric or skew-symmetric, since it is the eigenvector of the symmetric (nearly) centrosymmetric matrix $\mathbf{A}$ corresponding to the smallest eigenvalue. Oddly, it appears that the MSSNR-UNT TEQ is always symmetric as opposed to skew-symmetric, and the point of symmetry is not necessarily in the center of the impulse response.

To quantify the symmetry of the finite-length MSSNR-UNT TEQ design for various parameter values, we computed the TEQ for carrier serving area (CSA) test loops [26] 1 through 8, using TEQ lengths $3 \le \tilde{L}_w \le 40$. For each TEQ, we decomposed $\mathbf{w}$ into $\mathbf{w}_{\text{sym}}$ and $\mathbf{w}_{\text{skew}}$, then computed $\|\mathbf{w}_{\text{skew}}\|^2/\|\mathbf{w}_{\text{sym}}\|^2$. A plot of this ratio (averaged over the eight channels) for the MSSNR-UNT TEQ is shown in Figure 3. The symmetric part of each TEQ was obtained by considering all possible points of symmetry and choosing the one for which the norm of the symmetric part divided by the

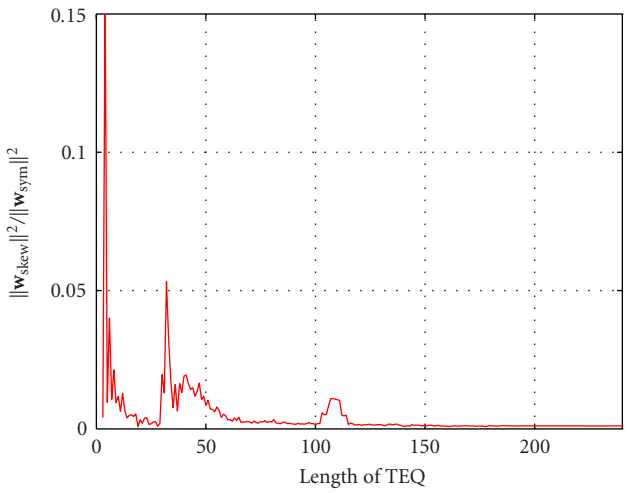

FIGURE 3: Energy in the skew-symmetric part of the TEQ over the energy in the symmetric part of the TEQ, for $\nu = 32$. The data was delay-optimized and averaged over CSA test loops from 1 to 8.

norm of the perturbation was maximized. For example, if the TEQ were $\mathbf{w} = [1, 2, 4, 2.2]$, then $\mathbf{w}_{\text{sym}} = [0, 2.1, 4, 2.1]$ and $\mathbf{w}_{\text{skew}} = [1, -0.1, 0, 0.1]$. The value of Δ was the delay which maximized the shortening SNR. The point of Figure 3 is not to prove that the infinite-length MSSNR-UNT TEQ is symmetric (that will be addressed in Section 5.2), but rather to give an idea of how quickly the finite-length design becomes symmetric.

Observe that the MSSNR-UNT TEQ (Figure 3) becomes increasingly symmetric for large TEQ lengths. For parameter values that lead to highly symmetric TEQs, the TEQ can be initialized by only computing half of the TEQ coefficients. For MSSNR, MSSNR-UNT, and MMSE solutions, this effectively reduces the problem from finding an eigenvector (or generalized eigenvector) of an $\hat{N} \times \hat{N}$ matrix to finding an eigenvector (or generalized eigenvector) of a $\lceil \hat{N}/2 \rceil \times \lceil \hat{N}/2 \rceil$ matrix, as shown in [23], where we use $\hat{N}$ to mean $\tilde{L}_w$ for the MSSNR TEQ computation and to mean ν for the MMSE TIR computation. This leads to a significant reduction in complexity, at the expense of throwing away the skew-symmetric portion of the filter. Reduced complexity algorithms are discussed in Section 6.

5.2. Infinite-length symmetry results

This section examines the limiting behavior of $\mathbf{A}$ and $\mathbf{B}$, and the resulting limiting behavior of the eigenvectors of $\mathbf{A}$ (i.e., the MSSNR-UNT solution). We will show that

$$\lim_{L_w \to \infty} \frac{\|\mathbf{H}^T\mathbf{H} - \mathbf{A}\|_F}{\|\mathbf{A}\|_F} = 0, \tag{31}$$

where $\|\cdot\|_F$ denotes the Frobenius norm [27]. Since $\mathbf{H}^T\mathbf{H}$ is symmetric and Toeplitz (and thus centrosymmetric), its eigenvectors are symmetric or skew-symmetric. Thus, as $L_w \to \infty$, we can expect the eigenvectors of $\mathbf{A}$ to become symmetric or skew-symmetric. Although this is a heuristic argument, the more rigorous $\sin(\theta)$ theorem[1] [28] is difficult to apply.

First, consider a TEQ that is finite, but very long. Specifically, we make the following assumptions:

A1: $\Delta > L_h > \nu$,
A2: $L_w > \Delta + \nu$.

Such a large Δ in A1 is reasonable when the TEQ length is large. Now, we can partition $\mathbf{H}$ as

$$\mathbf{H} = \begin{bmatrix} \mathbf{H}_1 & \mathbf{H}_{L2} & \mathbf{H}_{L1} & \mathbf{0} & \mathbf{0} \\ \mathbf{0} & \mathbf{H}_{U3} & \mathbf{H}_M & \mathbf{H}_{L3} & \mathbf{0} \\ \mathbf{0} & \mathbf{0} & \mathbf{H}_{U1} & \mathbf{H}_{U2} & \mathbf{H}_2 \end{bmatrix}. \tag{32}$$

The row blocks have heights Δ, $(\nu+1)$, and $(L_h + L_w - \nu - \Delta)$; and the column blocks have widths $(\Delta - L_h)$, $(\nu + 1)$, $(L_h - \nu - 1)$, $(\nu + 1)$, and $(L_w - \nu - \Delta)$. The sections $[\mathbf{H}_{L2}, \mathbf{H}_{L1}]$ and $\mathbf{H}_{L3}$ are both lower triangular and contain the "head" of the channel, $[\mathbf{H}_{U1}, \mathbf{H}_{U2}]$ and $\mathbf{H}_{U3}$ are both upper triangular and contain the "tail" of the channel, $\mathbf{H}_1$ and $\mathbf{H}_2$ are tall channel convolution matrices, and $\mathbf{H}_M$ is Toeplitz. Then $\mathbf{H}_{\text{win}}$ is simply the middle row (of blocks) of $\mathbf{H}$, and $\mathbf{H}_{\text{wall}}$ is the concatenation of the top and bottom rows.

Under the two assumptions above, $\mathbf{H}_{U3}$, $\mathbf{H}_M$, and $\mathbf{H}_{L3}$ will be constant for all values of Δ and L_w. As such, the limiting behavior of $\mathbf{B} = \mathbf{H}_{\text{win}}^T\mathbf{H}_{\text{win}}$ is

$$\begin{aligned} \mathbf{B} &= [\mathbf{0}, \mathbf{H}_{U3}, \mathbf{H}_M, \mathbf{H}_{L3}, \mathbf{0}]^T [\mathbf{0}, \mathbf{H}_{U3}, \mathbf{H}_M, \mathbf{H}_{L3}, \mathbf{0}] \\ &\triangleq \left[\mathbf{0}, \overline{\mathbf{H}}_3^T, \mathbf{0}\right]^T \left[\mathbf{0}, \overline{\mathbf{H}}_3^T, \mathbf{0}\right], \end{aligned} \tag{33}$$

where $\overline{\mathbf{H}}_3$ is a size $(\nu + \tilde{L}_h) \times (\nu + 1)$ channel convolution matrix formed from $\mathbf{Jh}$, the time-reversed channel. Since $\mathbf{B}$ is a zero-padded version of $\overline{\mathbf{H}}_3\overline{\mathbf{H}}_3^T$, it has the same Frobenius norm. Also, the values of L_w and Δ affect the size of the zero matrices in (33) but not $\overline{\mathbf{H}}_3$ (assuming that our assumptions hold), so L_w and Δ do not affect the Frobenius norm of $\mathbf{B}$. Therefore,

$$\|\mathbf{B}\|_F^2 = \text{constant} \triangleq B_F \tag{34}$$

whenever our two initial assumptions A1 and A2 are met.

The limiting behavior for $\mathbf{A}$ is determined by noting that

$$\mathbf{A} = \begin{bmatrix} \mathbf{H}_1^T\mathbf{H}_1 & \cdots & \mathbf{0} \\ \mathbf{H}_{L2}^T\mathbf{H}_1 & \cdots & \mathbf{0} \\ \mathbf{H}_{L1}^T\mathbf{H}_1 & \cdots & \mathbf{H}_{U1}^T\mathbf{H}_2 \\ \mathbf{0} & \cdots & \mathbf{H}_{U2}^T\mathbf{H}_2 \\ \mathbf{0} & \cdots & \mathbf{H}_2^T\mathbf{H}_2 \end{bmatrix}. \tag{35}$$

[1] The $\sin(\theta)$ theorem is a commonly used bound on the angle between the eigenvector of a matrix and the corresponding eigenvector of the perturbed matrix. This bound is a function of the eigenvalue separation of the matrix, which is not explicitly known in our problem; hence, the theorem cannot be directly applied.

(Only the top-left and bottom-right blocks are of interest for the proof.) Thus, a lower bound on the Frobenius norm of $\mathbf{A}$ can be found as follows:

$$\begin{aligned}\|\mathbf{A}\|_F^2 &\geq \left\|\mathbf{H}_1^T\mathbf{H}_1\right\|_F^2 + \left\|\mathbf{H}_2^T\mathbf{H}_2\right\|_F^2 \\ &\geq \|\mathbf{h}\|_2^4 \cdot \left((\Delta - L_h) + (L_w - \nu - \Delta)\right) \\ &= \|\mathbf{h}\|_2^4 \cdot (L_w - L_h - \nu),\end{aligned} \tag{36}$$

which goes to infinity as $L_w \to \infty$. In the second inequality, we have dropped all of the terms in the Frobenius norms except for those due to the diagonal elements of $\mathbf{H}_1^T\mathbf{H}_1$ and $\mathbf{H}_2^T\mathbf{H}_2$.

Now, let $\mathbf{C} \triangleq \mathbf{H}^T\mathbf{H}$, and recall from (14) that $\mathbf{C} = \mathbf{A} + \mathbf{B}$. Thus,

$$\frac{\|\mathbf{C} - \mathbf{A}\|_F^2}{\|\mathbf{A}\|_F^2} = \frac{\|\mathbf{B}\|_F^2}{\|\mathbf{A}\|_F^2} \leq \frac{B_F}{\|\mathbf{h}\|_2^4 \cdot (L_w - (L_h + \nu))}, \tag{37}$$

which goes to zero as $L_w \to \infty$. Thus, in the limit, $\mathbf{A}$ approaches $\mathbf{C}$, which is a symmetric centrosymmetric matrix. Heuristically, this suggests that in the limit, the eigenvectors of $\mathbf{A}$ (including the MSSNR-UNT solution) will be symmetric or skew-symmetric. However, for special cases (such as tridiagonal matrices), the eigenvector corresponding to the smallest eigenvalue is always symmetric as opposed to skew-symmetric [23]. Every single MSSNR TEQ that we have observed for ADSL channels has been nearly symmetric rather than skew-symmetric, suggesting (not proving) that the infinite length TEQ will be exactly symmetric. Thus, constraining the finite-length solution to be symmetric is expected to entail no significant performance loss, which is supported by simulation results. Essentially, if $\mathbf{v}$ is an eigenvector in the eigenspace of the smallest eigenvalue, then $\mathbf{Jv}$ is as well (where $\mathbf{J}$ is the matrix with ones on the cross diagonal and zeros elsewhere) so $(1/2)(\mathbf{v} + \mathbf{Jv})$ (which is symmetric) is as well, even if the smallest eigenvalue has multiplicity larger than 1.

Note that in the limit, $\mathbf{B}$ does not become centrosymmetric (refer to (33)), although it is approximately centrosymmetric about a point off of its center. Thus, we cannot make as strong of a limiting argument for the MSSNR solution as for the MSSNR-UNT solution. Symmetry in the finite-length MSSNR solution is discussed in [15].

6. EXPLOITING SYMMETRY IN TEQ DESIGN

In [15], it was shown that the MMSE target impulse response becomes symmetric as the TEQ length goes to infinity, and in Section 5.2, it was shown that the infinite-length MSSNR-UNT TEQ is an eigenvalue of a symmetric centrosymmetric matrix, and is expected to be symmetric. In [16, 17], simulations were presented for forcing the MSSNR TEQ to be perfectly symmetric or skew-symmetric. This section present algorithms for forcing the MMSE TIR to be exactly symmetric in the case of a finite length TEQ, and for forcing the MSSNR-UNT TEQ to be symmetric when it is computed in a blind, adaptive manner via the MERRY algorithm [10]. It is also shown that when the TEQ is symmetric, the TEQ and FEQ designs can be done independently (and thus in parallel).

Consider forcing the MSSNR-UNT TEQ to be symmetric as a means of reducing the computational complexity. The MSSNR-UNT TEQ arises, for example, in the MERRY algorithm [10], which is a blind, adaptive algorithm for computing the TEQ; or in the algorithm in [22] (if the constraint used is a UNT TEQ), which is a trained, iterative algorithm for computing the TEQ. We focus here on extending the MERRY algorithm to the symmetric case. Briefly, the idea behind the MERRY algorithm is that the transmitted signal inherently has redundancy due to the CP, so that redundancy should be evident at the receiver if the channel is short enough. The measure of redundancy is the MERRY cost,

$$J_{\text{MERRY}} = E\Big[\,\big|\,y(Mk + \nu + \Delta) - y(Mk + \nu + N + \Delta)\,\big|^2\Big], \tag{38}$$

where $M = N + \nu$ is the symbol length, k is the symbol index, and Δ is a user-defined synchronization delay. This cost function measures the similarity between a data sample and its copy in the CP (N samples earlier). The MERRY algorithm is a gradient descent of (38).

In practical applications, the TEQ length is even, due to a desired efficient use of memory. Thus, a symmetric TEQ has the form $\mathbf{w}^T = [\mathbf{v}^T, (\mathbf{Jv})^T]$. (An even TEQ length is not necessary; a similar partition can be made in the odd-length case, as will be done for the MMSE target impulse response later in this section.) The TEQ output is

$$y(Mk + i) = \sum_{j=0}^{L_w} w(j) \cdot r(Mk + i - j), \tag{39}$$

which can be rewritten for a symmetric TEQ as

$$\begin{aligned}&y(Mk + i) \\ &\quad = \sum_{j=0}^{\tilde{L}_w/2-1} v(j) \cdot \big(r(Mk + i - j) + r\big(Mk + i - L_w + j\big)\big).\end{aligned} \tag{40}$$

The Sym-MERRY update is a stochastic gradient descent of (38) with respect to the half-TEQ coefficients $\mathbf{v}$, with a renormalization to avoid the trivial solution $\mathbf{v} = \mathbf{0}$. See Algorithm 1 where

$$\begin{aligned}&\mathbf{u}(i) \\ &\quad = \left[r(i) + r(i - L_w), \ldots, r\left(i - \frac{\tilde{L}_w}{2} + 1\right) + r\left(i - \frac{\tilde{L}_w}{2}\right)\right]^T.\end{aligned} \tag{41}$$

Compared to the regular MERRY algorithm in [10], the number of multiplications has been cut in half for Sym-MERRY, though some additional additions are needed to

For symbol $k = 0, 1, 2, \ldots,$

$$\tilde{\mathbf{u}}(k) = \mathbf{u}(Mk + \nu + \Delta) - \mathbf{u}(Mk + \nu + N + \Delta),$$
$$e(k) = \mathbf{v}^T(k)\tilde{\mathbf{u}}(k),$$
$$\hat{\mathbf{v}}(k+1) = \mathbf{v}(k) - \mu e(k)\tilde{\mathbf{u}}^*(k),$$
$$\mathbf{v}(k+1) = \frac{\hat{\mathbf{v}}(k+1)}{||\hat{\mathbf{v}}(k+1)||_2}.$$

Algorithm 1

compute $\tilde{\mathbf{u}}$. Simulations of Sym-MERRY are presented in Section 7.

Now, consider exploiting symmetry in the MMSE target impulse response in order to reduce computational complexity. Recall that in the MMSE design, first, the TIR $\mathbf{b}$ is computed as the eigenvector of $\mathbf{R}(\Delta)$ [as defined in (11)], and then the TEQ $\mathbf{w}$ is computed from (8). The MSE (which we wish to minimize) is given by

$$E[e^2] = \mathbf{b}^T\mathbf{R}(\Delta)\mathbf{b}. \tag{42}$$

Typically, the CP length ν is a power of 2, so the TIR length $(\nu + 1)$ is odd. This is the case, for example, in ADSL [29], IEEE 802.11a [30] and HIPERLAN/2 [31] wireless LANs, and DVB [32]. To force a symmetric TIR, partition the TIR as

$$\mathbf{b}^T = [\mathbf{v}^T, \gamma, (\mathbf{J}\mathbf{v})^T], \tag{43}$$

where γ is a scalar and $\mathbf{v}$ is a real $(\nu/2)\times 1$ vector. Now rewrite the MSE as

$$[\mathbf{v}^T, \gamma, \mathbf{v}^T\mathbf{J}]\begin{bmatrix}\mathbf{R}_{11} & \mathbf{R}_{12} & \mathbf{R}_{13}\\ \mathbf{R}_{21} & \mathbf{R}_{22} & \mathbf{R}_{23}\\ \mathbf{R}_{31} & \mathbf{R}_{32} & \mathbf{R}_{33}\end{bmatrix}\begin{bmatrix}\mathbf{v}\\ \gamma\\ \mathbf{J}\mathbf{v}\end{bmatrix} = [\sqrt{2}\mathbf{v}^T, \gamma]\hat{\mathbf{R}}\begin{bmatrix}\sqrt{2}\mathbf{v}\\ \gamma\end{bmatrix}, \tag{44}$$

where

$$\hat{\mathbf{R}} = \begin{bmatrix}\frac{1}{2}(\mathbf{R}_{11} + \mathbf{R}_{13}\mathbf{J} + \mathbf{J}\mathbf{R}_{31} + \mathbf{J}\mathbf{R}_{33}\mathbf{J}) & \frac{1}{\sqrt{2}}(\mathbf{R}_{12} + \mathbf{J}\mathbf{R}_{32})\\ \frac{1}{\sqrt{2}}(\mathbf{R}_{21} + \mathbf{R}_{23}\mathbf{J}) & \mathbf{R}_{22}\end{bmatrix}. \tag{45}$$

For simplicity, let $\hat{\mathbf{v}}^T = [\sqrt{2}\mathbf{v}^T, \gamma]$. In order to prevent the all-zero solution, the nonsymmetric TIR design uses the constraint $\|\mathbf{b}\| = 1$. This is equivalent to the constraint $\|\hat{\mathbf{v}}\| = 1$. Under this constraint, the TIR that minimizes the MSE must satisfy

$$\hat{\mathbf{R}}\hat{\mathbf{v}} = \lambda\hat{\mathbf{v}}, \tag{46}$$

where λ is the smallest eigenvalue of $\hat{\mathbf{R}}$. Since both $\mathbf{R}$ and $\hat{\mathbf{R}}$ are symmetric, solving (46) requires 1/4 as many computations as solving the initial eigenvector problem. However, the forced symmetry could, in principle, degrade the performance of the associated TEQ. Simulations of the Sym-MMSE algorithm are presented in Section 7.

Another advantage of a symmetric TEQ is that it has a linear phase with known slope, allowing the FEQ to be designed in parallel with the TEQ. A symmetric TEQ can be classified as either a type I or type II FIR linear phase system [33, pages 298–299]. Thus, for a TEQ with $L_w + 1$ taps, the transfer function has the form

$$W(e^{j\omega}) = M(\omega)\exp\left(-j\frac{L_w}{2}\omega + j\beta\right), \tag{47}$$

where $M(\omega) = M(-\omega)$ is the magnitude response. The DC response is

$$M(0)e^{j\beta} = \sum_{k=0}^{L_w} w(k). \tag{48}$$

Since the TEQ is real, $e^{j\beta}$ must be real, so

$$\beta = \begin{cases}0, & \sum_k w(k) > 0,\\ \pi, & \sum_k w(k) < 0.\end{cases} \tag{49}$$

If $\sum_k w(k) = 0$, the DC response does not reveal the value of β. In this case, one must determine the phase response at another frequency, which is more complicated to compute. The response at $\omega = \pi$ is fairly easy to compute and will also reveal the value of β.

From (47), (48), and (49), given the TEQ length, the phase response of a symmetric TEQ is known up to the factor $e^{j\beta}$, even before the TEQ is designed. The phases of the FEQs are then determined entirely by the channel phase response. Thus, if a channel estimate is available, the two possible FEQ phase responses could be determined in parallel with the TEQ design. Similarly, if the TIR is symmetric and the TEQ is long enough that the TIR and effective channel are almost identical, then the phase response of the effective channel is known, except for β. If differential encoding is used, then the value of β can arbitrarily be set to either 0 or π since a rotation of exactly 180 degrees does not affect the output of a differential detector. Furthermore, if 2-PAM or 4-QAM signaling is used on a subcarrier, the magnitude of the FEQ does not matter, and the entire FEQ for that tone can be designed without knowledge of the TEQ.

For an ADSL system, 4-QAM signaling is used on all of the subcarriers during training. Thus, the FEQ can be designed for the training phase by only setting its phase response. The magnitude response can be set after the TEQ is designed. The benefit here is that if the FEQ is designed all at once (both magnitude and phase), then a division of complex numbers is required for each tone. However, if the phase response is already known, determining the FEQ magnitude only requires a division of real numbers for each tone. This can allow for a more efficient implementation.

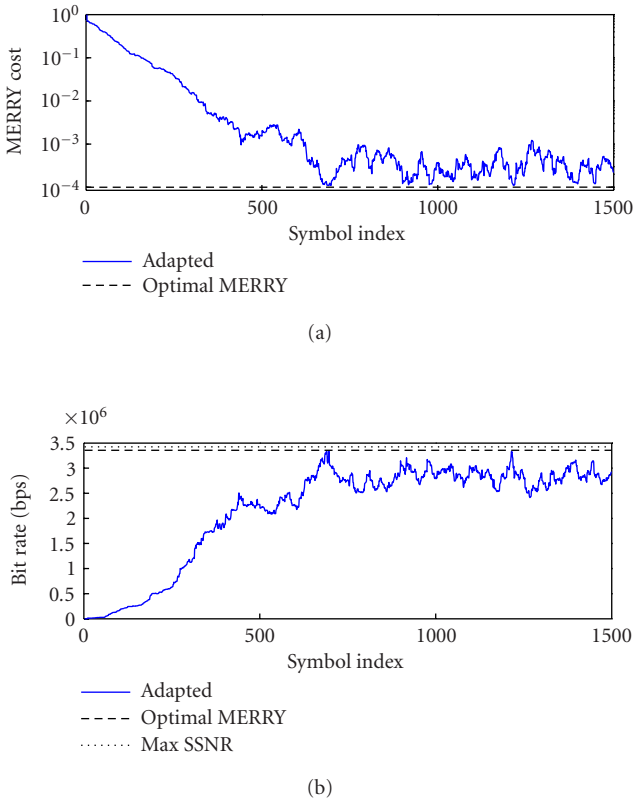

Figure 4: Performance of Sym-MERRY versus time for CSA loop 4. (a) MERRY cost. (b) Achievable bit rate.

7. SIMULATIONS

This section presents simulations of the Sym-MERRY and Sym-MMSE algorithms. The parameters used for the Sym-MERRY algorithm were an FFT of size $N = 512$, a CP length of $\nu = 32$, a TEQ of length $\tilde{L}_w = 16$ (8 taps get updated, then mirrored), and an SNR of $\sigma_x^2\|\mathbf{h}\|^2/\sigma_n^2 = 40$ dB, with white noise. The channel was CSA loop 4 (available at [34]). The DSL performance metric is the achievable bit rate for a fixed probability of error

$$B = \sum_i \log_2\left(1 + \frac{\mathrm{SNR}_i}{\Gamma}\right), \tag{50}$$

where SNR_i is the signal to interference and noise ratio in frequency bin i. (We assume a 6 dB margin and 4.2 dB coding gain; for more details, refer to [9].) Figure 4 shows performance versus time as the TEQ adapts. The dashed line represents the solution obtained by a nonadaptive solution to the MERRY cost (38), without imposing symmetry, and the dotted line represents the performance of the MSSNR solution [5]. Observe that Sym-MERRY rapidly obtains a near-optimal performance. The jittering around the asymptotic portion of the curve is due to the choice of a large step size.

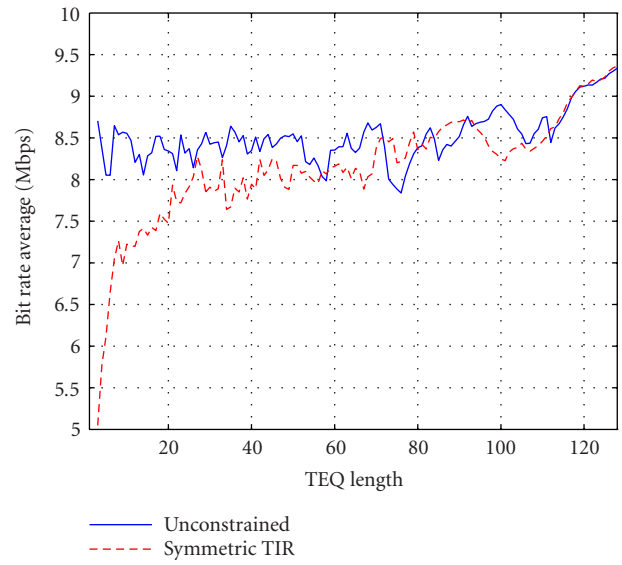

Figure 5: Achievable bit rate in Mbps of MMSE (solid) and Sym-MMSE (dashed) designs versus TEQ length, averaged over eight CSA test loops.

Table 4: Achievable bit rate (Mbps) for MMSE and Sym-MMSE, using 20-tap TEQs and 33-tap TIRs. The last column is the performance of the Sym-MMSE method in terms of the percentage of the bit rate of the MMSE method. The channel has an additive white Gaussian noise but no crosstalk.

Loop #	MMSE	Sym-MMSE	Relative
CSA1	8.6323	7.9343	91.91%
CSA2	9.1396	9.1721	100.36%
CSA3	8.5877	8.3360	97.07%
CSA4	8.3157	5.6940	68.47%
CSA5	8.4821	6.3433	74.78%
CSA6	8.8515	9.0016	101.70%
CSA7	7.5244	5.8360	77.56%
CSA8	7.2037	7.4878	103.94%

The simulations for the Sym-MMSE algorithm are shown in Figure 5 and in Table 4. In Figure 5, TEQs were designed for CSA loops from 1 to 8, then the bit rates were averaged. The TEQ lengths that were considered were $3 \le \tilde{L}_w \le 128$. For TEQs with fewer than 20 taps, the bit rate performance of the symmetric MMSE method is not as good as that of the unconstrained MMSE method. However, asymptotically, the results of the two methods agree; and for some parameters, the symmetric method achieves a higher bit rate. Table 4 shows the individual bit rates achieved on the 8 channels using 20 tap TEQs, which is roughly the boundary between good and bad performance of the Sym-MMSE design in Figure 5. On average, for a 20-tap TEQ, the Sym-MMSE method achieves 89.5% of the bit rate of the MMSE method, with a significantly lower computational cost, but

the performance (at this filter length) varies significantly depending on the channel. Thus, it is suggested that the symmetric MMSE design should only be used for TEQs with at least 20 taps, and preferably more than that.

8. CONCLUSIONS

The computational complexity of two popular channel shortening algorithms, the MSSNR and MMSE methods, has been addressed. A method was proposed which reduces the complexity of computing the **A** and **B** matrices in the MSSNR design by a factor of 140 (for typical ADSL parameters) compared to the methods of Wu et al. [8], for a total reduction of a factor of 4000 compared to the brute force approach, without degrading performance. A similar technique was proposed to reduce the complexity of computing the $\mathbf{R}(\Delta)$ matrix used in the MMSE design by a factor of 16 (for typical ADSL parameters). It was also shown that the infinite length MSSNR TEQ with a unit norm TEQ constraint has a symmetric impulse response. Algorithms for reducing complexity by exploiting symmetry in the TEQ and target impulse response were derived, and simulations were used to show that the symmetric algorithms incur only a minor performance penalty. The Matlab code to reproduce the figures in this paper is available online at http://bard.ece.cornell.edu/matlab/martin/index.html.

ACKNOWLEDGMENTS

The authors wish to thank Mr. Milos Milosevic of The University of Texas at Austin and Mr. Andrew Klein and Mr. John Walsh of Cornell University for their comments. This work was supported in part by Applied Signal Technology (Sunnyvale, CA), the Olin Fellowship from Cornell University, and The State of Texas Advanced Technology Program under Project 003658-0614-2001.

REFERENCES

[1] A. N. Akansu, P. Duhamel, X. Lin, and M. de Courville, "Orthogonal transmultiplexers in communication—A review," *IEEE Trans. Signal Processing*, vol. 46, no. 4, pp. 979–995, 1998.

[2] N. Al-Dhahir and J. M. Cioffi, "Efficiently computed reduced-parameter input-aided MMSE equalizers for ML detection: A unified approach," *IEEE Transactions on Information Theory*, vol. 42, no. 3, pp. 903–915, 1996.

[3] D. D. Falconer and F. R. Magee, "Adaptive channel memory truncation for maximum likelihood sequence estimation," *Bell System Technical Journal*, vol. 52, no. 9, pp. 1541–1562, 1973.

[4] N. Al-Dhahir and J. M. Cioffi, "Optimum finite-length equalization for multicarrier transceivers," *IEEE Trans. Communications*, vol. 44, no. 1, pp. 56–64, 1996.

[5] P. J. W. Melsa, R. C. Younce, and C. E. Rohrs, "Impulse response shortening for discrete multitone transceivers," *IEEE Trans. Communications*, vol. 44, no. 12, pp. 1662–1672, 1996.

[6] D. Daly, C. Heneghan, and A. D. Fagan, "A minimum mean-squared error interpretation of residual ISI channel shortening for discrete multitone transceivers," in *Proc. IEEE Int. Conf. Acoustics, Speech, Signal Processing (ICASSP '01)*, vol. 4, pp. 2065–2068, Salt Lake City, Utah, USA, May 2001.

[7] B. Farhang-Boroujeny and M. Ding, "Design methods for time-domain equalizer in DMT transceivers," *IEEE Trans. Communications*, vol. 49, no. 3, pp. 554–562, 2001.

[8] J. Wu, G. Arslan, and B. L. Evans, "Efficient matrix multiplication methods to implement a near-optimum channel shortening method for discrete multitone transceivers," in *Proc. 34th IEEE Asilomar Conference on Signals, Systems, and Computers (Asilomar '00)*, vol. 1, pp. 152–157, Pacific Grove, Calif, USA, October–November 2000.

[9] G. Arslan, B. L. Evans, and S. Kiaei, "Equalization for discrete multitone receivers to maximize bit rate," *IEEE Trans. Signal Processing*, vol. 49, no. 12, pp. 3123–3135, 2001.

[10] R. K. Martin, J. Balakrishnan, W. A. Sethares, and C. R. Johnson Jr., "A blind, adaptive TEQ for multicarrier systems," *IEEE Signal Processing Letters*, vol. 9, no. 11, pp. 341–343, 2002.

[11] M. Milosevic, L. F. C. Pessoa, B. L. Evans, and R. Baldick, "Optimal time domain equalization design for maximizing data rate of discrete multi-tone systems," to appear in *IEEE Trans. Signal Processing*.

[12] K. Vanbleu, G. Ysebaert, G. Cuypers, M. Moonen, and K. Van Acker, "Bitrate maximizing time-domain equalizer design for DMT-based systems," submitted to *IEEE Trans. Communications*.

[13] G. D. Forney, "Maximum-likelihood sequence estimation of digital sequences in the presence of intersymbol interference," *IEEE Transactions on Information Theory*, vol. 18, no. 3, pp. 363–378, 1972.

[14] I. Medvedev and V. Tarokh, "A channel-shortening multiuser detector for DS-CDMA systems," in *Proc. 53rd Vehicular Technology Conference (VTC '01)*, vol. 3, pp. 1834–1838, Rhodes, Greece, May 2001.

[15] R. K. Martin, M. Ding, B. L. Evans, and C. R. Johnson Jr., "Infinite length results and design implications for time-domain equalizers," to appear in *IEEE Trans. Signal Processing*.

[16] C. Ribeiro, V. Silva, and P. S. R. Diniz, "Impulse response shortening for xDSL discrete multitone modems with linear phase filters," in *II Conferencia Internacional de Telecomunicaciones y Electrónica (TELEC '02)*, Santiago de Cuba, Cuba, July 2002.

[17] C. Ribeiro, V. Silva, and P. S. R. Diniz, "Linear phase impulse response shortening for xDSL DMT modems," in *Proc. IEEE International Telecommunications Symposium (ITS '02)*, Natal, Brazil, September 2002.

[18] J. M. Cioffi, "A multicarrier primer," ANSI TIE1.4 Committee Contribution, No. 91-157, November 1991, http://www.stanford.edu/~cioffi/.

[19] K. Van Acker, G. Leus, M. Moonen, O. van de Wiel, and T. Pollet, "Per tone equalization for DMT-based systems," *IEEE Trans. Communications*, vol. 49, no. 1, pp. 109–119, 2001.

[20] C. Yin and G. Yue, "Optimal impulse response shortening for discrete multitone transceivers," *Electronics Letters*, vol. 34, no. 1, pp. 35–36, 1998.

[21] M. H. Hayes, *Statistical Digital Signal Processing and Modeling*, John Wiley & Sons, New York, NY, USA, 1996.

[22] M. Nafie and A. Gatherer, "Time-domain equalizer training for ADSL," in *Proc. IEEE International Conference on Communications (ICC '97)*, vol. 2, pp. 1085–1089, Montreal, Quebec, Canada, June 1997.

[23] A. Cantoni and P. Butler, "Eigenvalues and eigenvectors of symmetric centrosymmetric matrices," *Linear Algebra and Its Applications*, vol. 13, no. 3, pp. 275–288, 1976.

[24] A. Cantoni and P. Butler, "Properties of the eigenvectors of persymmetric matrices with applications to communication theory," *IEEE Trans. Communications*, vol. 24, no. 8, pp. 804–809, 1976.
[25] J. Makhoul, "On the eigenvectors of symmetric Toeplitz matrices," *IEEE Trans. Acoustics, Speech, and Signal Processing*, vol. 29, no. 4, pp. 868–872, 1981.
[26] K. Sistanizadeh, "Loss characteristics of the proposed canonical ADSL loops with 100-Ohm termination at 70, 90, and 120 F," ANSI T1E1.4 Committee Contribution, No. 161, November, 1991.
[27] G. H. Golub and C. F. Van Loan, *Matrix Computations*, Johns Hopkins University Press, Baltimore, Md, USA, 3rd edition, 1996.
[28] C. Davis and W. Kahan, "The rotation of eigenvectors by a perturbation. III," *SIAM Journal on Numerical Analysis*, vol. 7, no. 1, pp. 1–46, 1970.
[29] T. Starr, J. M. Cioffi, and P. T. Silverman, *Understanding Digital Subscriber Line Technology*, Prentice-Hall PTR, Upper Saddle River, NJ, USA, 1999.
[30] The Institute of Electrical and Electronics Engineers, "Wireless LAN Medium Access Control (MAC) and Physical Layer (PHY) Specifications," IEEE Standard 802.11a, 1999.
[31] The European Telecommunication Standards Institute, "Broadband Radio Access Networks (BRAN); High Performance Radio Local Area Networks (HIPERLAN) Type 2; System Overview," ETR101 683 114, 1999.
[32] The European Telecommunication Standards Institute, "Digital Video Broadcasting (DVB); Framing Structure, Channel Coding and Modulation for Digital Terrestrial Television," ETSI EN 300 744 V1.4.1, 2001.
[33] A. V. Oppenheim and R. W. Schafer, *Discrete-Time Signal Processing*, Prentice-Hall, Upper Saddle River, NJ, USA, 2nd edition, 1998.
[34] G. Arslan, M. Ding, B. Lu, M. Milosevic, Z. Shen, and B. L. Evans, *The University of Texas at Austin. Matlab DMTTEQ toolbox version 3.1*, http://www.ece.utexas.edu/~bevans/projects/adsl/dmtteq/dmtteq.html.

Richard K. Martin obtained dual B.S. degrees in physics and electrical engineering from the University of Maryland, College Park in 1999 (Summa Cum Laude) and an M.S. in electrical engineering from Cornell University in 2001. He is pursuing his Ph.D. in electrical engineering in Cornell University. His research interests include equalization for multicarrier systems; blind, adaptive algorithms; reduced complexity equalizer design; and exploiting sparsity for performance improvement of adaptive filters. He has had five journal papers and twelve conference papers accepted for publication. He is a lead author of the book *Theory and Design of Adaptive Filters Answer Book*, and he has three pending patents.

Ming Ding received his B.S. degree from the Department of Electronic Science at Nankai University in 1995 and his M.E. degree from the Department of Electrical and Computer Engineering at National University of Singapore in 1999, respectively. From 1995 to 1997, Ming had been an R&D Engineer with the National Post and Telecommunications Industry Corporation (PTIC), Shanghai. From April 1999 to August 2000, he has been working as an R&D Engineer for the Centre for Wireless Communications at the National University of Singapore. Ming is currently a full-time Ph.D. student in electrical engineering at the University of Texas at Austin. Since 2001, he has been a Research Assistant with Embedded Signal Processing Laboratory at The University of Texas at Austin. During summers, he serves among the co-op student staff at DSPS R&D Center, Texas Instruments, Dallas. During Fall 2002, he was a nondegree graduate student at Cornell University. His current research interests include multicarrier modulation, channel equalization, and adaptive filtering with applications in broadband wireless and wireline communications.

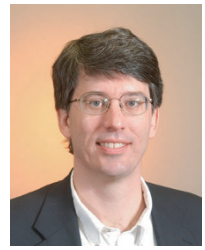

Brian L. Evans received his BSEECS degree from the Rose-Hulman Institute of Technology in May 1987, and his MSEE and Ph.D.EE degrees from Georgia Institute of Technology in December 1988 and September 1993, respectively. From 1993 to 1996, he was a Postdoctoral Researcher in design automation for embedded systems in the Department of EECS, University of California, Berkeley. From 1996 to 2000, he was an Assistant Professor in the Department of Electrical and Computer Engineering (ECE) at The University of Texas at Austin. Since 2000, he has been an Associate Professor of ECE at UT Austin. In Fall 2002, he spent a revitalizing sabbatical at Cornell University with Professor Rick Johnson's research group. His research interests include the design and embedded real-time software implementation of high data rate equalizers for ADSL/VDSL transceivers, high-quality halftoning for desktop printers, smart image acquisition for digital still cameras, and high-resolution 3D sonar imaging systems. Professor Evans has published over 100 refereed conference and journal papers. Professor Evans is a member of the Design and Implementation of Signal Processing Systems Technical Committee of the IEEE Signal Processing Society, and a recipient of the 1997 US National Science Foundation CAREER Award.

C. Richard Johnson Jr. was born in Macon, GA in 1950. He is currently a Professor of electrical and computer engineering at Cornell University, Ithaca, NY. Professor Johnson received the Ph.D. degree in electrical engineering with minors in engineering-economic systems and art history from Stanford University in 1977. In 1989, he was elected a Fellow of the IEEE "for contributions to adaptive parameter estimation theory with applications in digital control and signal processing." Since then, his primary research interest has been blind adaptive fractionally-spaced linear and decision feedback equalization for intersymbol and structured multiuser interference removal from single and multicarrier communication systems. His research group's activity is currently supported by the National Science Foundation, Applied Signal Technology, and Texas Instruments.